Atomic Layer Deposition and Vapor Deposited SAMS in a CrossBeam FIB-SEM Platform: A Path To Advanced Materials Synthesis

E. L. Principe†, Cheryl Hartfield‡, Rocky Kruger‡, Aaron Smith‡, Ray Dubois, Kirk Scammon**, Brian Kempshall****
†Carl Zeiss SMT, Inc.‡ Omniprobe, Inc., Colonial Metals, Inc.**, University of Central Florida, NanoSpective****
eprincipe01@hotmail.com

Introduction

Nanopatterning refers to the fabrication of nanometer-scale structures, meaning patterns with at least one lateral dimension between the size of an individual atom and approximately 100 nm. *Direct Write or Maskless Lithography* as discussed in this article refers to the use of a focused beam, either an ion beam or an electron beam, to create a patterned image directly into (etch), or on top of (deposition), the target material. Both electron beams and ion beams can be used together with gas injection technology to deposit three dimensional structures on the nanometer scale through the process of either electron beam assisted or ion beam assisted chemical vapor deposition (CVD). The deposition occurs only in the vicinity where the electron beam or ion beam is being scanned. Therefore, the deposit will follow the form of the scanned beam in two dimensions. This approach can be applied to produce three-dimensional objects by successively layering upon the two-dimensional pattern. In the case of ion beams in particular, the direct write process can also produce an etch pattern on the nanometer scale as the ion beam physically mills away the material via ion bombardment. This process can also be chemically enhanced for certain materials such as simultaneous use of water to selectively etch carbon.

The FIB-SEM platform is already unrivaled in the variety of top-down and bottom-up[i] nanopatterning that can be accomplished within one compact environment. However, these platforms have yet unrealized potential in the role of "reaction chamber." Fulfilling this potential will enable a wider variety of bottom-up processing in the FIB-SEM environment. In turn, this leads to even broader applications in prototyping, as well as research combining nanopatterning with advanced materials synthesis. While the universal molecular assembler may still be far into the realm of fantasy, the more practical goal of improving the range and quality of processing and synthesis that can be completed within the FIB-SEM is a critical evolutionary step to create a more comprehensive and programmable nanopatterning engine. Here, we demonstrate the feasibility of atomic layer deposition (ALD) and vapor deposition of self-assembled monolayers (SAMS) within a Zeiss CrossBeam™ FIB-SEM vacuum chamber in an effort to extend the functional envelope of the typical FIB-SEM platform.

Historically, the chemical deposition reactions performed in a commercial FIB-SEM platform have been limited to a relatively small suite of common precursors and minor variants using either ion- or electron-beam assisted chemical vapor deposition (CVD). To a large extent, the freedom to develop more sophisticated thin film processes in the FIB-SEM platform has been limited by the gas injection system (GIS) hardware and software used for precursor and reactive gas delivery. The simplest form of GIS consists of (1) a crucible containing a precursor material, which is typically heated or cooled to form the desired vapor pressure and (2) a capillary operated by an open/shut type of valve, which introduces the vapor into the vacuum chamber. A GIS suitable for advanced processing should also permit mass flow control of all constituent precursors, as well as a capacity for mixing carrier and reactive gases. Mass flow

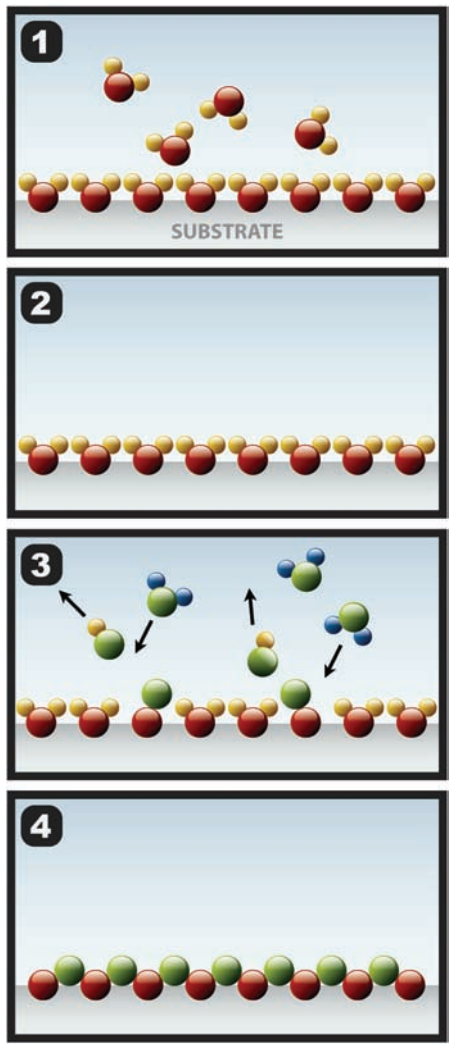

Figure 1: Schematic representation of the ALD process. 1) chemisorption of reactant "A" 2) saturation, 3) chemical reaction between reaction "A" and "B" where volatiles are pumped away, 4) final product.

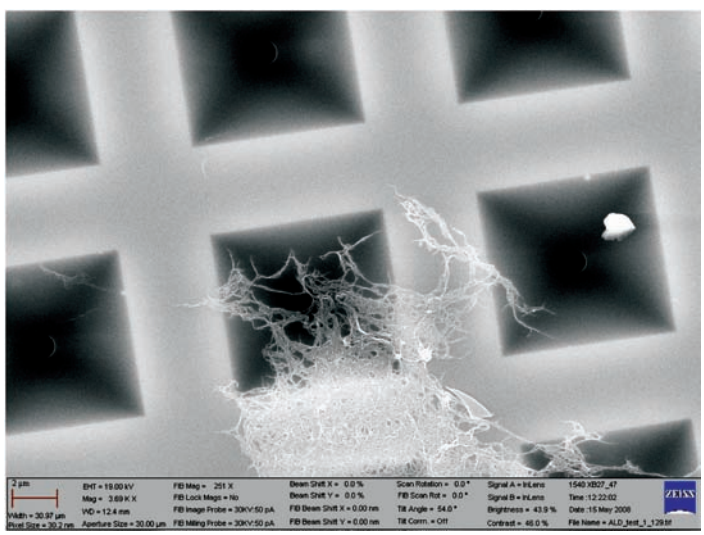

Figure 2: Typical distribution of CNTs on the TEM membrane following evaporation. The CNTs were distributed across several sections of the grid.

i Top-down and bottom-up processing with respect to nanotechnology are two approaches for the manufacture of products. Bottom-up approaches often use molecular components to build more complex assemblies. The top-down approach uses methods to cut, mill and shape materials into the desired shape and order. Micropatterning techniques, such as photolithography and inkjet printing belong to this category. Bottom-up approaches, in contrast, use the chemical properties of single molecules to cause single-molecule components to (a) self-organize or self-assemble into some useful conformation, or (b) rely on positional assembly. These approaches utilize the concepts of molecular self-assembly.

NEW

OmniGIS™

Multi-Source Gas Injection System for the FIB & SEM

FEATURES:

- Programmable Process Flows
- Feedback Control
- Single Needle Delivery
- Fast & Easy Crucible Replacement
- Economical

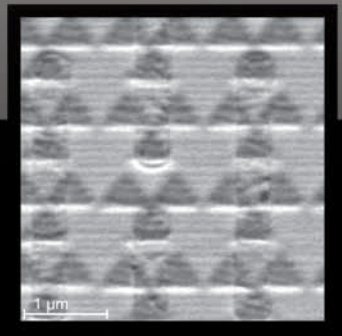

Make

FIB deposited plasmonic nanostructures

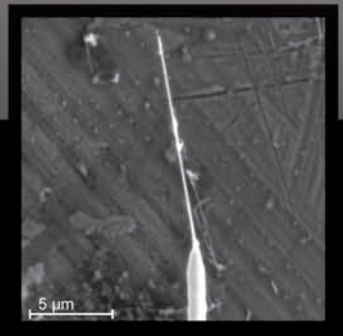

Move

Single nanowire analysis

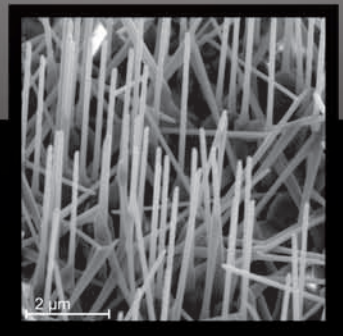

Modify

Chemical surface alteration

For more information visit us at **http://www.omniprobe.com** or call us at **214.570.6800.**

omniprobe

www.omniprobe.com

control is critical for tuned delivery of chemical reactants, process repeatability, and uniformity. Another key feature is software architecture to permit recipe-based automation through creation and recall of complex process flows. Process flows may incorporate repeated cycling of several precursor and carrier gas mixtures. Sequential cycling of precursors with precise flow control and carrier gas mixing is exactly what is required to enable epitaxial-type depositions such as ALD in a FIB-SEM environment (GIS-ALD). A capability to work equally well with liquid mixtures or solid precursors broadens applications to include GIS vapor deposited SAMS (GIS-SAMS) and delivery of other functionalized molecular systems. These systems, which have utility both as patterning templates and photoresist, can now also be considered for use within the FIB-SEM platform. It is only recently that ALD and SAMS deposition in a FIB-SEM could be explored, due to the availability of a GIS system fulfilling all the key requirements. Combined with ancillary components such as stage heating and plasma etching, novel structures can be produced.

GIS-ALD Experiments

ALD is a self-limiting sequential chemical reaction that deposits conformal, pin-hole free thin films of materials onto substrates with varying compositions, surface topographies, and aspect ratios. Invented in 1974 by Dr. Tuomo Suntola, ALD is similar in chemistry to CVD except that the ALD reaction breaks the CVD reaction into two half-reactions[1]. The process is represented schematically in **Figure 1**. Reactant "A" chemisorbs onto the surface to saturation. Reactant "B" then chemically reacts with "A" leaving a uniform layer of the product on the surface while the volatile components of the reaction are pumped away. The cycle then repeats. Precursor materials are kept separate during the respective reaction phases. Each set of gas pulses (one cycle) produces a consistent fractional monolayer increase in film thickness. Thus, the resulting film thickness may be precisely controlled with atomic layer precision by varying the number of deposition cycles. The semiconductor industry has held tremendous interest in ALD technology for CMOS high-*k* gate dielectric semiconductors, as well as DRAM capacitors and non-Si device gate dielectrics. ALD is becoming the method of choice for other industries also, driven in large part by the demands of nanotechnology. Features of commercial ALD systems include: relatively high chamber pressures, ranging from the upper mTorr up to 1-5 Torr; gas purging between reactants (typically using Ar or N_2); and often high temperatures (200-400C is required to achieve vapor phase at high pressures), though room temperature and low temperature chemistries do exist. The premise of this work is that ALD-type growth can be implemented in FIB-SEM instruments via sequential GIS technology. Local gas injection means the overall chamber vacuum is still approximately 10^{-5} Torr and is high only in the local area where the deposition is concentrated.

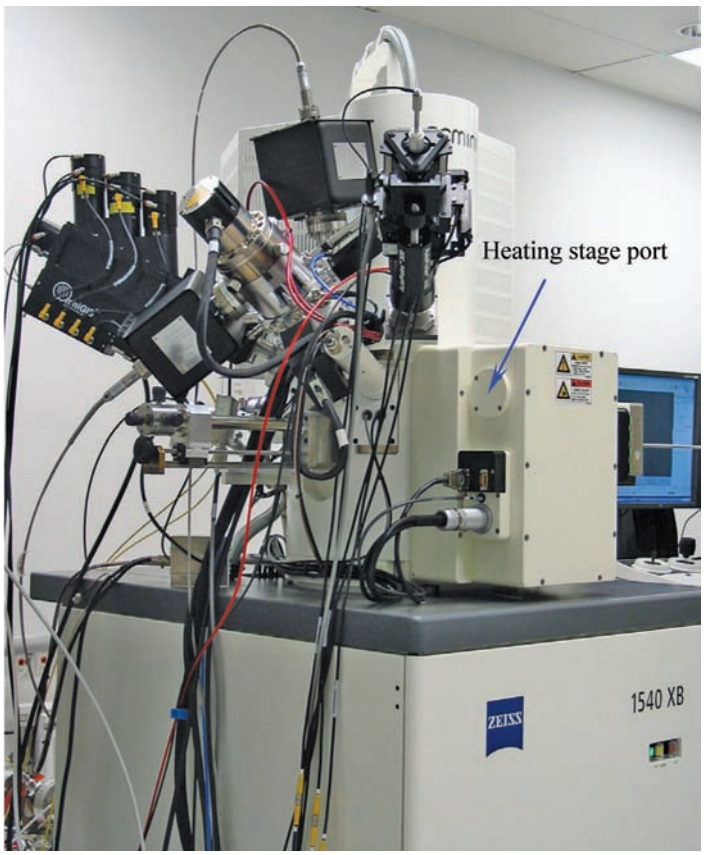

Figure 3: CrossBeam configuration used in GIS-ALD and GIS-SAMS experiments. Heating stage leads connected through the port indicated by the arrow in the figure.

Figure 4: The single GIS nozzle extends from the right in the image and is directed through a circular opening on the lid of the heater substage. The heater substage acts as a gas concentrator for the GIS-ALD experiments.

Experimental

Materials:

Carbon nanotubes (CNTs) were chosen as the ALD substrate. The single-walled carbon nanotubes (SWNT) were fabricated by a

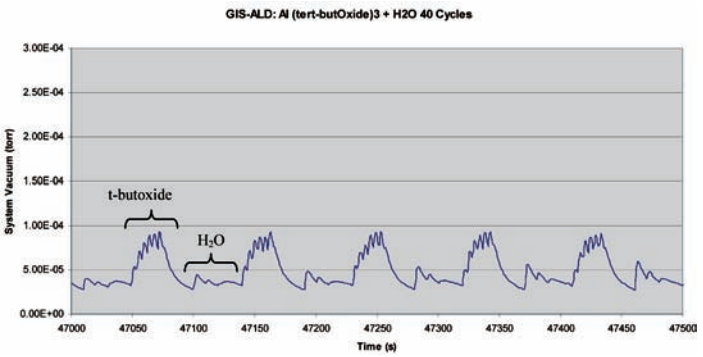

Figure 5: An excerpt from the pressure fluctuation timeline during the GIS-ALD testing on t-butoxide. The periods associated with the t-butoxide and water cycles are evident. The individuals pulses observed (6 for t-butoxide and 3 for H_2O) are determined by the duty cycle in the GIS recipe.

Side-By-Side Comparison? Difficult When Our Coaters Stand Alone.

High Resolution Sputter Coater 208HR for FE-SEM

Superior Features:

- High Resolution Fine Coating
- Wide Choice of Coating Materials
- High Resolution Thickness Control
- Multiple Sample Stage Movements
- Wide Range of Operating Pressures
- Compact, Modern, Benchtop Design

Find out about our complete line of sample coaters.

TED PELLA, INC.
Microscopy Products for Science and Industry

4595 Mountain Lakes Blvd., Redding, CA 96003-1448
Phone: 530-243-2200 or 800-237-3526 (USA) FAX: 530-243-3761
Email: sales@tedpella.com Web Site: www.tedpella.com

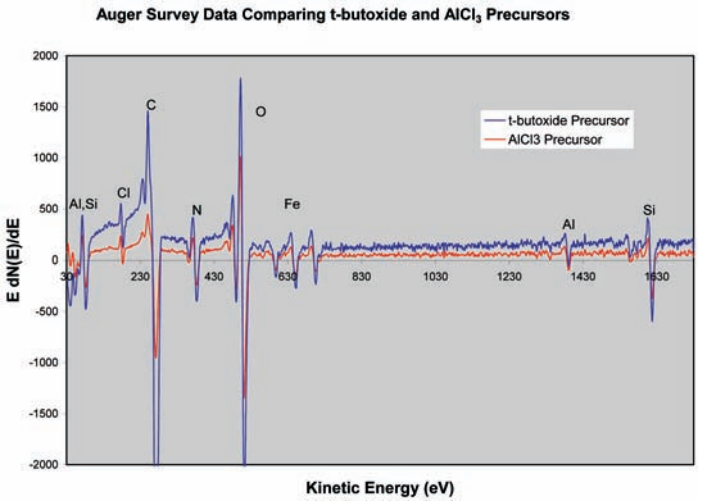

Figure 6: Auger data from substrates processed with both precursors indicated the presence of aluminum on the CNTs. As the analysis was over a large area, the silicon and nitrogen signals from the TEM membrane are also observed.

high pressure carbon monoxide process (HiPCO) and suspended in MeOH. A drop of the suspension was placed on a ProtoChips DuraSiN™ grid and allowed to air dry. A representative sample is shown in **Figure 2**. The CNTs tend to aggregate into bundles when prepared in this manner. Placing the CNTs directly on a TEM grid allowed TEM inspection of post-ALD samples without further sample preparation. Aluminum oxide was chosen as the ALD deposition material using a recipe modified from that of Farmer, *et al.*[2] An oxide was selected for initial testing in particular, because deionized water is the common source of O_2 for the secondary reaction product. Aluminum tert-butoxide ($C_{12}H_{27}AlO_3$ or tert-$(butO)_3Al$) was one of two aluminum oxide precursors tested. The other precursor was aluminum trichloride, $AlCl_3$. Both of these chemicals were supplied courtesy of Colonial Metals, Inc.

Equipment:

Tests were conducted at Omniprobe facilities using a Zeiss 1540 CrossBeam™ Platform configured with a Gemini electron column, Canion ion column, 5 element STEM detector, Omniprobe AutoProbe™ 300 nanomanipulator, XEI Scientific Evactron plasma cleaner, an E.F. Fullam heating stage and Omniprobe OmniGIS™ gas injection system. The OmniGIS™ features multiple gases delivered on a single port with programmable feedback control, single needle delivery, and drag and drop recipe creation for running complex process flows. The system configuration is shown in **Figure 3**.

Methods:

Prior to ALD deposition, SWNTs require a pretreatment to make them reactive to ALD chemistries. Farmer et al. showed that one can create a "glue layer" by room temperature pretreatment of SWNTs with repeated cycles of NO_2 and NO_x species to form a monolayer ring around the CNTs. The CNTs in this study were exposed to a slightly different nitrogen-based pretreatment than in the referenced work[2]. The first step consisted of 20 cycles of N_2O for 15 seconds at room temperature. This was followed by 30 alternating cycles of N_2O and tert-$(butO)_3Al$ at room temperature with each cycle taking 1.5 minutes. Then, the substrate temperature was ramped to 240°C and an additional 133 cycles of tert-$(butO)_3Al$ and H_2O were applied. The process finished with 15 cycles of H_2O. The entire sequence of pretreatment, main ALD deposition cycles, and finish cycles can be saved within one base recipe to be recalled and executed automatically in the future. Likewise, it is possible to create virtually any combination of process flows and repeat those flows as many times as desired. Based upon ~0.9 Å/cycle for this process, the total thickness is estimated at ~12 nm. The $AlCl_3$ process used a different source of NO_x, concentrated liquid nitric oxide. The pretreatment and finish cycles were the same, but the main process consisted of just 25 cycles for the ALD deposition. The time allotted for the chemical exposure during each cycle was intentionally much longer than typically required for conventional ALD. This was done to ensure sufficient time for saturation of the self-limiting process. It is expected that considerably shorter exposure cycles can be applied with the same result. The gases were also concentrated in the region of the substrate that was attached to the heater substage. The sample was positioned on the recessed heating element and covered with a small plate containing a ~20mm diameter hole. The GIS nozzle was inserted through the hole in proximity to the sample. The arrangement is shown in **Figure 4**.

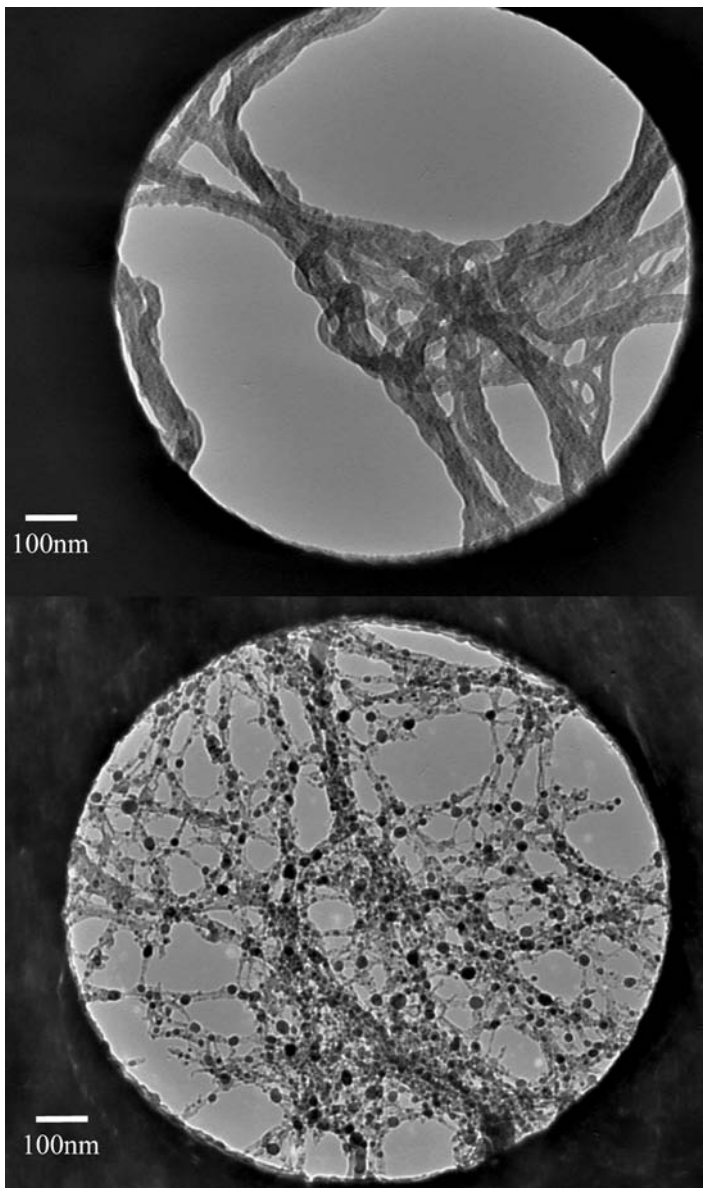

Figure 7: The low magnification brightfield TEM image of CNTs processed using the t-butoxide precursor shows a uniform coating (top). An image acquired under identical conditions and magnification of CNTs processed using the $AlCl_3$ precursor indicates a nonuniform coating (bottom). See text for details.

MIRA\\ Schottky FE-SEM

Value and Excellence in SEMs

www.tescan.com

- Wide Field Optics™
- In-Flight Beam Tracing™
- In-Beam Detector
- Active Vibration Isolation

All as Tescan standard for the highest-quality imaging

TESCAN
PERFORMANCE IN NANOSPACE

Tescan USA Inc.
Web: www.tescan-usa.com
Email: info@tescan-usa.com
Tel: 724-772-7433

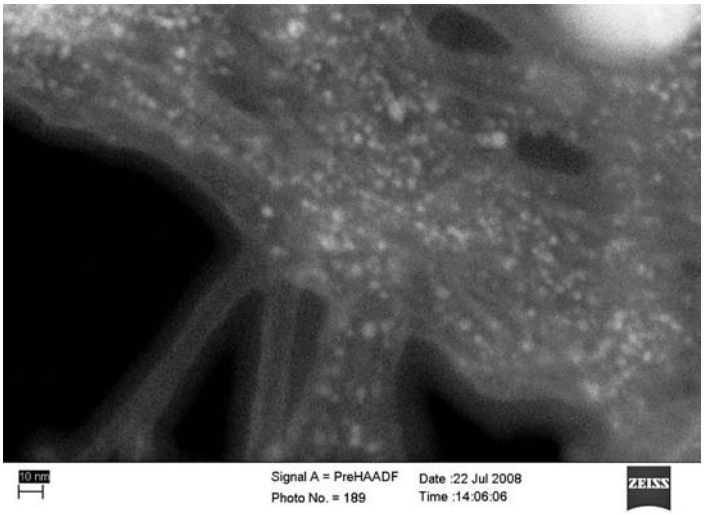

Figure 8: Bright particles representing the iron catalyst are visible in this high angle annular dark field STEM image of a section of bundled CNTs that was GIS-ALD processed using t-butoxide and water. The lower left portion of the image contains a branch of CNTs low in catalyst density. The ALD coating on this branch is on the order of 10nm in thickness.

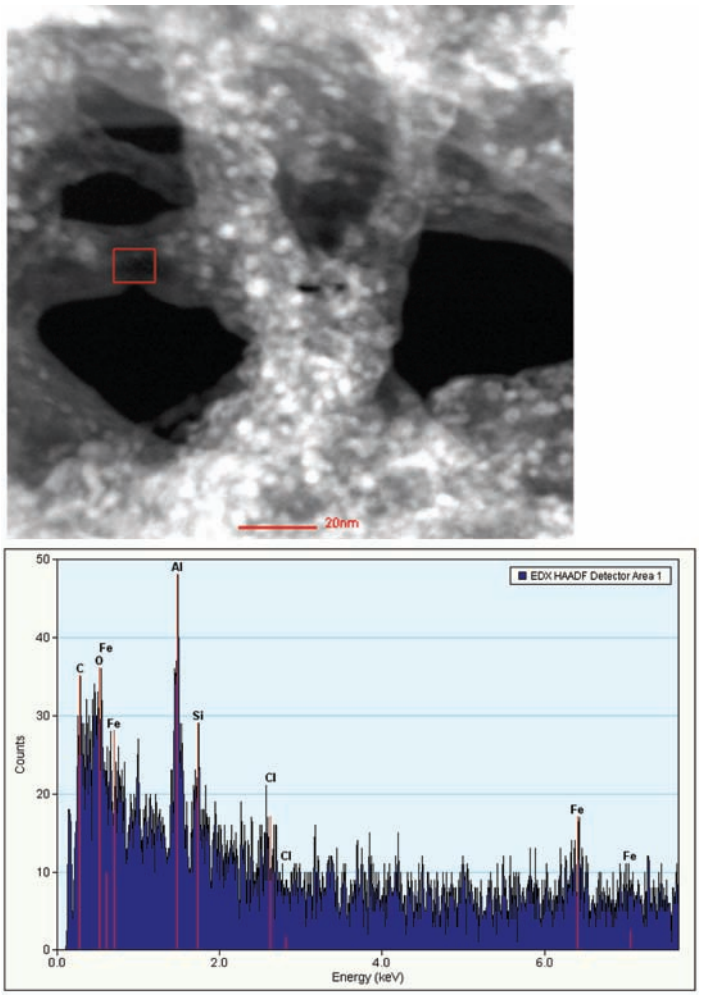

Figure 9: Area XEDS analysis from CNTs processed by GIS-ALD using a t-butoxide precursor and water oxygen source. The analysis taken from the rectangular region shown above confirms a coating containing aluminum and oxygen. It can not be verified from the data that a stoichiometric aluminum oxide has been produced.

Again, this measure was taken to enhance the local gas pressure, but it is not necessarily a requisite for the deposition to succeed. It is likely sufficient to place the sample on the heating element completely open to system vacuum. Pressure variations associated with the GIS pulses were tracked using the CrossBeam's built-in system pressure monitor during the deposition process.

It should be emphasized that in these tests the electron and ion columns were isolated from the system vacuum during the entire deposition process, and the substrate surface was never exposed to ion beam or electron beam bombardment prior to the deposition. The process is entirely chemically driven. However, the opportunity to modify the surface with either the ion beam or the electron beam is one of the *primary motivations* for conducting a deposition in a FIB-SEM platform and is the subject of our future tests. The incubation period is a well-known characteristic of ALD deposition, and that behavior is highly sensitive to the surface chemistry. Modification of the surface chemistry via an energy beam (ion, electron, photon) could either enhance or inhibit growth locally depending upon the reaction. This is a potential route to direct-write patterned ALD and other patterned synthesis. Integrating *in-situ* surface modification via ions, electrons, photons, etc., with epitaxial deposition methods such as described here is a tremendous opportunity.

Results

A time plot showing the system pressure variation associated with each cycle from the tert-butoxide ALD precursor is shown in **Figure 5**. The repeating pattern is evident where the portions of the trace associated with the t-butoxide and the water are marked in the figure. There are six controlled pulses within each t-butoxide cycle and three controlled pulses associated with each water cycle. The pulse frequency controls the duty cycle and is part of the GIS pre-programmed recipe designed and executed by the operator. The pressure sensor is an effective means to monitor the process and verify GIS operation. The GIS system can also employ a residual gas analyzer (RGA) to provide direct feedback on the chemical reactants in real-time during the recipe. This feature is especially useful to conduct more detailed studies and ensure tight compositional process control.

Initially, Auger analysis was conducted over a 50μm^2 area on the samples exposed to the Al (t-butOx)$_3$ and the $AlCl_3$ precursor chemistries. Auger data in **Figure 6** clearly show aluminum present on the SWNT bundles from both precursors. Silicon and nitrogen are associated with the nitride window on the TEM grid, and iron is associated with the catalyst material in the CNTs. Primarily, the Auger confirms the presence of aluminum on and around the CNTs. The $AlCl_3$ precursor suggested a higher concentration of aluminum despite a much lower total number of cycles, presuming all else was equal. However, comparing the low magnification brightfield TEM images in **Figure 7** reveals the tert-(butO)$_3$Al precursor chemistry produced an even film over the SWNT bundles, while the $AlCl_3$ precursor produced a "splotchy" deposit. Both images depict coated CNTs fibers randomly strewn across an open hole in the TEM membrane and are shown at the same scale. Comparing the two images in Figure 7, it is clear the CNTs in the tert-butoxide ALD process are uniformly "dilated," and the branches are generally much thicker with respect to the CNTs from the splotchy $AlCl_3$ process. Reasons for the splotchy coating are not clear without further testing, but may be associated with the use of NO_x gas evolved from the nitric acid liquid precursor. This was quite aggressive and may have compromised the process. Further analysis was directed toward the nature of the even film produced from the tert-butoxide precursor. A higher magnification high-angle annular dark-field STEM image in

Figure 8 depicts a section of the aggregated SWNTs where the bright regions represent the iron catalyst particles. The lower left portion of the image shows two branches of CNTs primarily devoid of iron catalyst material and shows a uniform coating approximately 10nm in thickness surrounding both branches, in reasonable agreement with the estimated thickness based upon the number of cycles. Finally, **Figure 9** shows image data matched with the XEDS data from the analysis area depicted and confirms the coating surrounding the bundles is comprised of aluminum and oxygen. The combined data show successful pretreatment and subsequent reaction with the ALD chemistries to form a coating on the SWNTs.

GIS-SAMS Experiments

In the 1940's, Zisman et al. discovered that an alkanoic acid could self-organize into a monolayer on a clean platinum surface driven by chemisorption from a solution phase.[3] The first gold-alkylthiolate monolayer was produced by Allara and Nuzzo at Bell laboratories in 1983.[4] Today, the many areas of SAM applications include biology, electrochemistry and electronics, nanoelectromechanical systems (NEMS) and microelectromechanical systems (MEMS), and everyday household goods. SAMs can serve as models for studying membrane properties of cells and organelles and cell attachment on surfaces. SAMs can also be used to modify the surface properties of electrodes for electrochemistry, general electronics, and various NEMS and MEMS (Love et al.).[5] Specific applications include uses as both positive and negative photoresist, and as an anti-stiction coating for MEMS. Rain-X is a household SAM product that keeps car windshields clear of rain by means of a hydrophobic monolayer. So, while it is clear that vapor deposited SAM have a host of commercial and research applications, it is not yet a common part of the GIS deposition repertoire. As it turns out, it is relatively easy to convey vapor deposited SAM via a GIS in a FIB-SEM.

Experimental

Materials:

Perflourooctlytrichlorosilane ($C_8H_4Cl_3F_{13}Si$), also known as FOTS, was chosen as the SAMs material. This organochlorosilane chemistry is an anti-stiction coating for MEMS devices. The substrate was a Si wafer with an approximately 1-μm thick blanket layer of Al-0.5% Cu (no Si doping).

Deposition conditions:

Prior to deposition, the substrate surface was cleaned using the Evactron system. Deposition occurred with the following GIS parameters: a 2% duty cycle, a period of 10s, and an "on" time of 0.2s. The carrier gas was N_2, delivered at 3 pulses/period. The SAMs crucible was cooled to 5°C, and the needle orifice positioned 50μm from the surface. The total run time was ~5 minutes. The GIS line pressure ranged from 1.2 to 0.4 mbar during the test.

Results

XPS survey analysis data is provided in Figure 10. Together with the high resolution multiplex spectra, the data indicates a deposition consistent with a flourosilane. Pending studies include analysis from a synchrotron-based large area imaging NEXAFS spectrometer to provide detailed information on both the spatial distribution and orientation of SAM deposited via the GIS.

Discussion and Conclusions

Current data suggest successful GIS-ALD deposition of aluminum oxide and GIS-SAM deposition of FOTS in a CrossBeam® FIB-SEM. To the authors' knowledge, this represents the first time these types of depositions have been performed in a FIB-SEM platform. The aggregation of the CNTs into bundles complicates the analysis and interpretation, and future work will benefit from performing studies on isolated fibers and other substrates. The methods described here provided a simple means to test the approach.

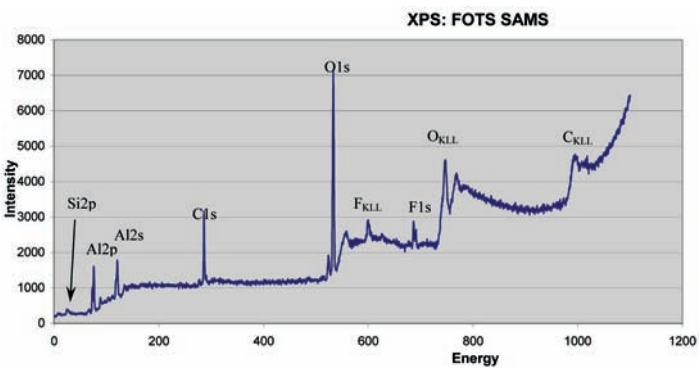

Figure 10: Large area (2mm x 2mm) XPS analysis of the GIS-SAMS sample processed using a FOTS source shows a deposit consistent with a fluorosilane.

These results provide proof of concept for an approach to create novel types of chemistries in a FIB-SEM environment. The possibility exists to extend the bottom-up process functionality of a FIB-SEM environment to include more advanced patterning and deposition methods through techniques like GIS-ALD and GIS-SAMS. The success of these initial experiments has broad implications for prototyping and future research involving advanced nanopatterning. Many additional GIS-ALD chemistries are possible candidates for OmniGIS™ delivery in the FIB-SEM, with applications in gate oxides, ferroelectrics, and metals. Likewise, other creative syntheses involving self-assembly are possible. There is a unique benefit conducting these experiments within the FIB-SEM environment, as the "blind watchmaker" issue can be avoided, since nanoscale imaging can be combined with patterning and deposition methods on the same scale. Future directions include patterned or direct-write ALD which will involve tailoring surface chemistries to promote or inhibit growth based upon interaction with energetic sources (electron, ion, photon, etc.). ■

Acknowledgements

The authors gratefully acknowledge David C. Bell & Alexander Orchowski for providing the TEM and STEM image data from the Libra 200 located at Harvard CNS, and Mikhail Kozlov at the Nanotechnology Institute at the University of Texas at Dallas for providing the SWNTs. We are also very grateful to Peter Kalu of Florida State University for loan of his heating stage for the ALD experiments, and we thank Earl Atnip of Texas Instruments for supplying the blanket aluminum wafer used for the SAM experiment.

References

1. Suntola, T., "Atomic Layer Epitaxy", *Thin Solid Films* 216, pp82-89 (1992)
2. Farmer, D. B. and R. G. Gordon (2006). "Atomic Layer Deposition on Suspended Single-Walled Carbon Nanotubes via Gas-Phase Noncovalent Functionalization." *NANO LETTERS* 6(4): 699-703
3. Biglow, W., D. Pickett, and W. Zisman, Oleophobic monolayers. I. Films Adsorbed From Solution In Non-Polar Liquids. *Journal of Colloid and Interface Science*, 1946. 1: p. 513-538
4. Nuzzo, R. G.; Allara, D. L., "Adsorption of Bifunctional Organic Disulfides on Gold Surfaces" *J. Am. Chem. Soc.* 1983, 105, 4481-4483
5. Love, J.C. *et al.* Self-Assembled Monolayers of Thiolates on Metals as a Form of *Nanotechnology. Chem. Rev.* 2005, 105, 1103-1169